Electronic Supplementary Information (ESI)

Rational Design, Synthesis, and Characterization of a Photocrosslinkable Hole-Transporting Polymer for High Performance Solution-Processed Thermally Activated Delayed Fluorescence OLEDs

Ji Hye Lee,[a] Cheol Hun Jeong,[a] Mallesham Godumala,[a] Chae Yeong Kim,[a] Hyung Jong Kim,[a] Jin Hyo Hwang,[a] Yong Woo Kim,[b] Dae Hyuk Choi,[b] Min Ju Cho*[a] and Dong Hoon Choi*[a]

[a] Department of Chemistry, Research Institute for Natural Sciences, Korea University, 145 Anam-ro, Seongbuk-gu, Seoul, 02841, Republic of Korea
[b] LT Materials, 113-19, Dangha-Ro, Namsa-Myeon, Cheoin-Gu, Yongin-Si, Gyeonggi-Do 17118, Korea.

E-mail: chominju@korea.ac.kr; dhchoi8803@korea.ac.kr

Experimental

Instrumental analysis

A Bruker 500-MHz spectrometer was utilized to acquire ^{1}H nuclear magnetic resonance (NMR) spectra. The number-average molecular weight of the newly synthesized **PX2Cz** was measured using gel-permeation chromatography (polystyrene standard and *o*-dichlorobenzene as the eluent at 80 °C with an Agilent GPC 1200 series instrument).

Differential scanning calorimetry (DSC) was employed to investigate the polymer thermal properties under a N_2 atmosphere, using a Mettler 821 instrument. Thermogravimetric analysis (TGA) was performed using a SCINCO TGA-N 1000 thermal-analysis system. Absorption spectroscopy was performed using a UV–vis absorption spectrometer (Agilent HP 8453, PDA-type) to prepare the film sample. The **PX2Cz** was dissolved in chlorobenzene, and the solution was deposited via spin-coating on a cleaned glass substrate. The films were photocured at elevated temperatures of 80, 100, and 120 °C for a fixed UV-irradiation time (10 s). Absorption spectroscopy was also used to investigate the solvent resistance after UV irradiation. The photocured films were rinsed with chloroform, and the absorption spectra were acquired sequentially. Cyclic voltammetry (CV) was performed using an eDAQ EA161 potentiostat (scan rate = 50 mV s^{-1}, reference electrode = Ag/AgCl, electrochemical workstation model). The sample was prepared by dissolving the **PX2Cz** in DCM (1.0 wt.%), and the solution was cast on a Pt plate. CV was performed before and after photocuring at 120 °C for 10 s.

Device fabrication

The fabrication process was performed by the following procedures. The ITO-coated glass substrate was successively pre-cleaned with deionized water and isopropanol. After drying at 100 °C overnight, PEDOT:PSS was deposited as an HIL, followed by annealing at 155 °C for 15 min. The **PX2Cz** solution in chlorobenzene was deposited by spin-coating and cured at 120 °C for 10 seconds and the PVK solution in chlorobenzene was spin-coated and annealed at 130 °C for 20 min. The emissive layer was

spin coated from a toluene solution made with IAPC and t4CzIPN, and then 2,2′,2″-(1,3,5-benzinetriyl)-tris(1-phenyl-1*H*-benzimidazole) (TPBi), LiF, and the Al electrode were prepared using the thermal evaporator. To find the best OLED performance conditions, we fabricated the devices at three di□erent dopant concentrations (i.e., 6, 9, and 12 wt %). We observed the current density−voltage−luminance (J−V−L) using a Keithley 236 source-measure unit instrument and a SpectraScan colorimeter (PR-655) using the devices fabricated above. All of the device performance measurements were carried out under ambient conditions.

Space-charge-limited current (SCLC) method for measuring hole mobility

The hole mobilities of the HTMs were measured using SCLC method after being fabricated in a typical device structure of ITO/PEDOT:PSS (40 nm)/as-cast or photocured **PX2Cz** or **PVK** film (100 nm)/MoO_3 (10 nm)/Ag (100 nm). The mobility was calculated according to $J = 9\varepsilon_0\varepsilon_r\mu V^2/8L^3$, where J is the current density; ε_0 is the permittivity of the HTL; ε_r is the relative dielectric constant; μ is the hole mobility; and L is the thickness of the HTL. The internal voltage is $V = V_{appl} - V_{bi} - V_a$, where V_{appl} is the voltage applied to the device; V_{bi} is related to the work-function difference between two electrodes; and V_a is the voltage drop.

Absorption and photoluminescence spectra of PX2Cz solution

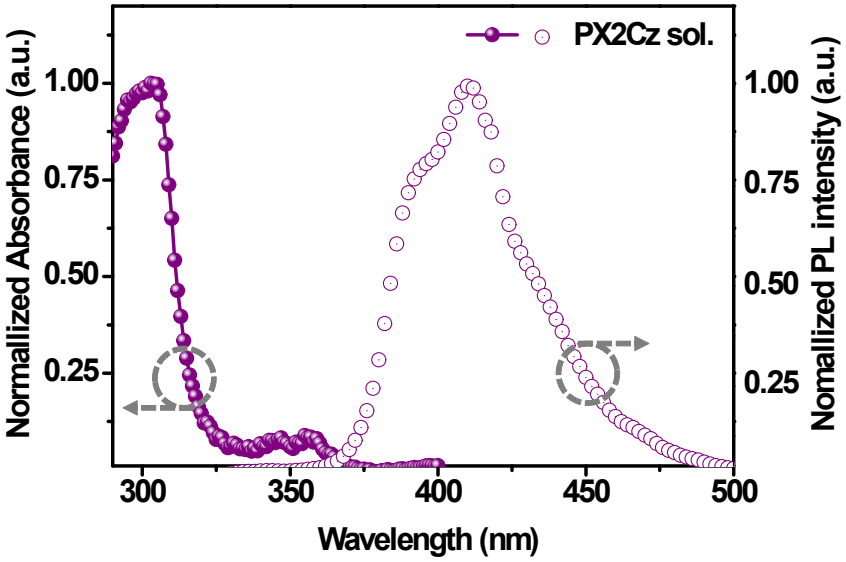

Figure S1. UV–vis absorption and photoluminescence (PL) spectra of **PX2Cz** in solution state.

Table S1. Optical and electrochemical properties of **PX2Cz** before and after photosensitive curing.

Sample	curing condition	λ_{max} [a] (nm)	λ_{onset} [a] (nm)	$E_g^{opt.}$ [b] (eV)	E_{ox} [c] (V)	Energy levels (eV)	
						HOMO [d]	LUMO [e]
As-cast film	-	307	374	3.32	0.94	−5.37	−2.05
Photocured film	120 °C, 10 s	307	374	3.32	0.94	−5.37	−2.05

[a] Film state. [b] $1240/\lambda_{onset}$. [c] The oxidation potentials were obtained from cyclic voltammograms in the film state. [d] HOMO = $-e(4.44\ V + E_{ox})$. [e] LUMO = (HOMO + E_g^{opt}).

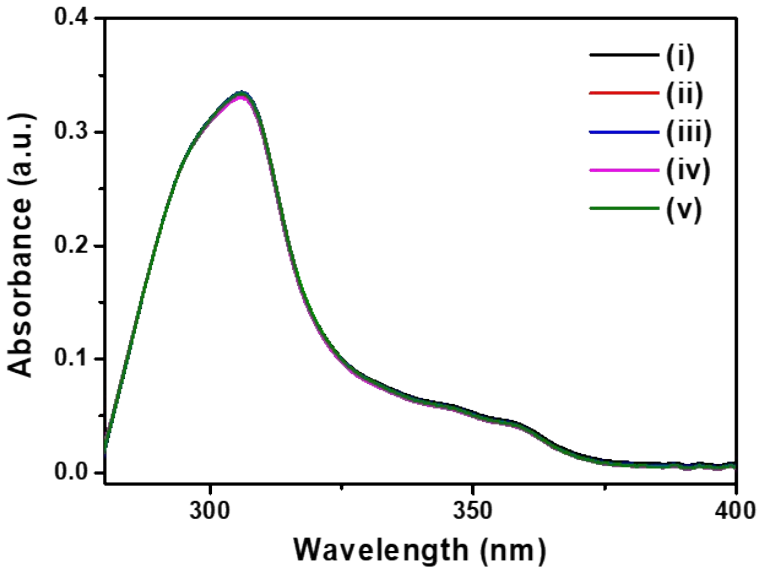

Figure S2. Absorption spectra of (i) photocured film and rinsed films (Rinsing time: (ii) 1 min, (iii) 2 min, (iv) 3min, (v) 5 min, respectively)

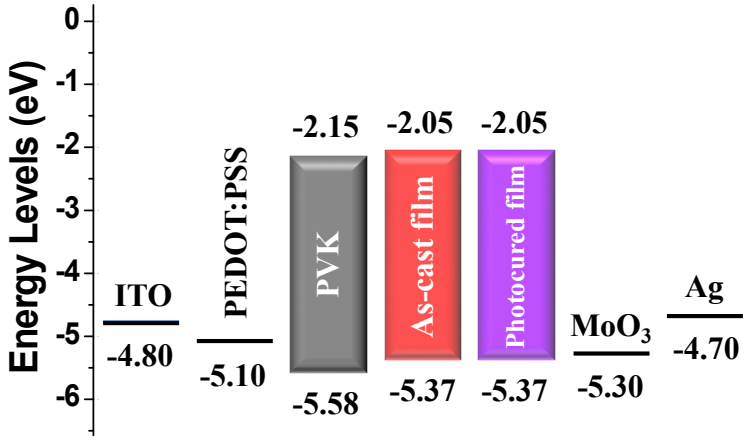

Figure S3. Energy-level diagram for hole-only device. (curing condition: 120 °C, 10 s UV-irradiation)

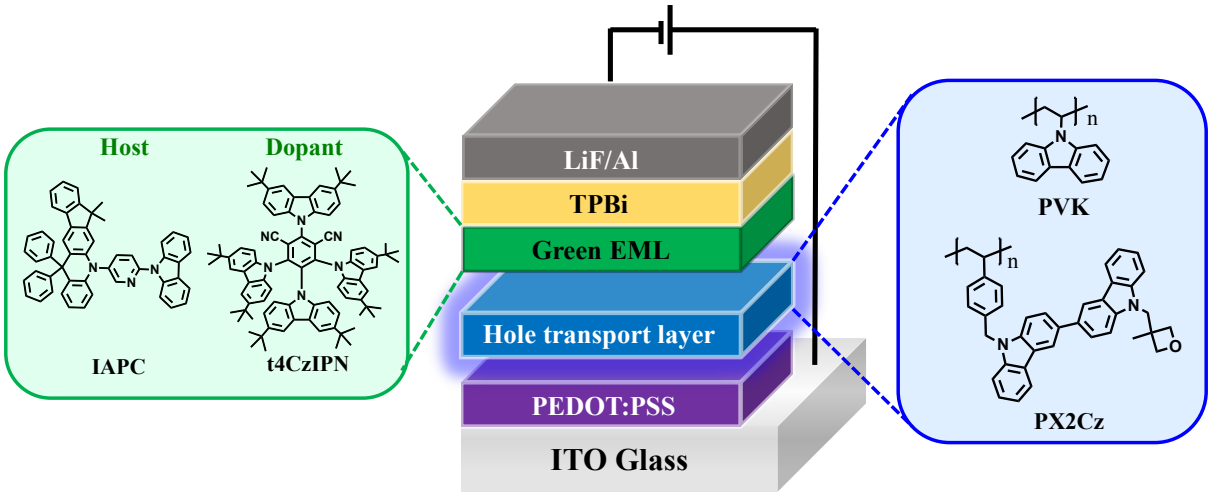

Figure S4. Device structure and materials for solution-processed green TADF-OLED.

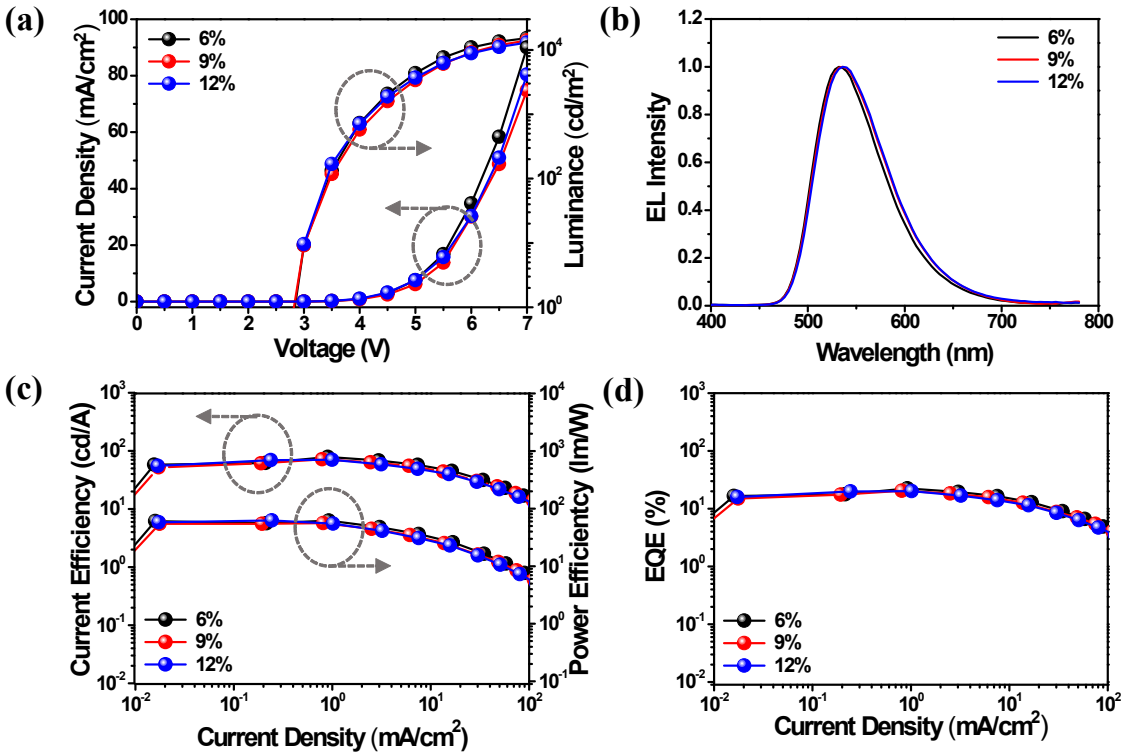

Figure S5. (a) Current density–voltage-luminance (*J*–*V*–*L*) curve, (b) EL spectra, (c) Current efficiency–luminance-power efficiency (CE–*L*–PE) curves, and (d) EQE–current density curves obtained from the optimized solution-processed green TADF OLED devices bearing photocured **PX2Cz** layer. *The doping concentration of the dopant in the EML was examined in the range of 6–12 wt.%.

Table S2. Performance of photocured **PX2Cz**-based green TADF-OLEDs with various dopant concentration in the EML.

HTM	Dopant concentration	V_{on} [a] (V)	CE_{max} [b] (cd/A)	PE_{max} [c] (lm/W)	Luminance [d] (cd/m^2)	EQE [e] (%)	CIE [f] (x, y)
PX2Cz	6%	2.8	78.9	61.9	16 000	22.5	(0.35,0.60)
PX2Cz	9%	2.8	71.4	56.1	15 700	20.4	(0.36,0.59)
PX2Cz	12%	2.8	70.0	62.2	14 200	20.1	(0.36,0.59)

[a.] Turn-on voltage at 1 cd/m^2, [b.] Maximum current efficiency. [c.] Maximum power efficiency. [d.] Maximum luminance. [e.] Maximum external quantum efficiency. [f.] Commission Internationale de L'Eclairage coordinates at 1000 cd m^{-2}.

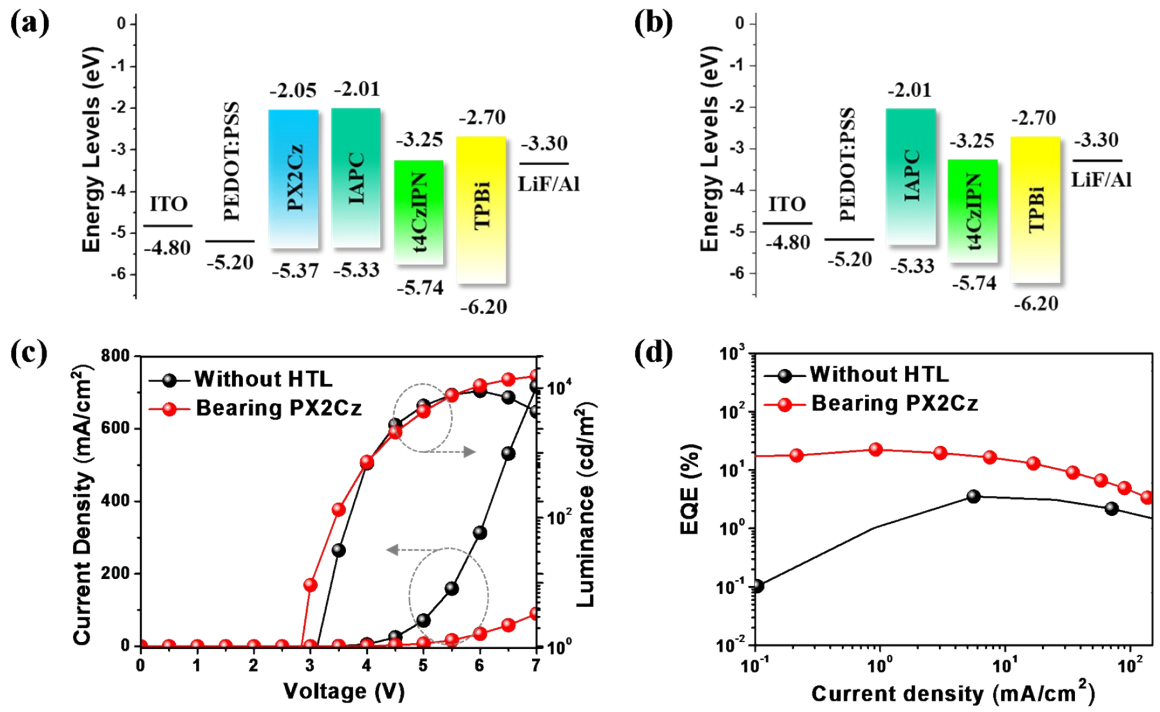

Figure S6. Energy level diagram of green TADF-OLEDs device with **PX2Cz** HTL (a) and without HTL (b) and Current density–voltage-luminance (J-V-L) curve (c), EQE–current density curves (d) obtained from the optimized solution-processed green TADF OLED devices with and without HTL.

Table S3. Performance of green TADF-OLED devices with and without HTL.

Device	Dopant concentration	V_{on} [a] (V)	CE_{max} [b] (cd/A)	PE_{max} [c] (lm/W)	Luminance [d] (cd/m^2)	EQE [e] (%)	CIE [f] (x, y)
w/o HTL	6%	3.0	12.30	9.66	9,000	3.52	(0.33, 0.60)
w/ HTL	6%	2.6	78.86	61.94	15,900	22.50	(0.35,0.60)

[a.] Turn-on voltage at 1 cd/m^2, [b.] Maximum current efficiency. [c.] Maximum power efficiency. [d.] Maximum luminance. [e.] Maximum external quantum efficiency. [f.] Commission Internationale de L'Eclairage coordinates at 1000 cd m^{-2}.